Geotechnical Testing Journal

doi:10.1520/GTJ20180218 / Vol. 43 / No. 2 / 2020 / available online at www.astm.org

Yongmin Kim,[1] Harianto Rahardjo,[2] and Nguyen Cong Thang[1]

Elastoplastic Behavior of Compacted Kaolin under Consolidated Drained and Shearing Infiltration Conditions

Reference

Y. Kim, H. Rahardjo, and N. C. Thang, "Elastoplastic Behavior of Compacted Kaolin under Consolidated Drained and Shearing Infiltration Conditions," *Geotechnical Testing Journal* 43, no. 2 (March/April 2020): 414–435. https://doi.org/10.1520/GTJ20180218

ABSTRACT

This study presents a comprehensive laboratory study to characterize the elastoplastic behavior of compacted kaolin under consolidated drained (CD) and shearing-infiltration (SI) triaxial conditions. The laboratory tests include a soil-water characteristic curve (SWCC), isotropic consolidation (IC), CD, and SI tests under different net confining stresses to consider in situ stress state and matric suctions that describe the volume change characteristics of unsaturated soil with respect to two stress state variables (i.e., net normal stress and matric suction). Consistently prepared specimens of statically compacted kaolin were used in this study. The results of the SWCC tests demonstrated that the air-entry value and yield suction (s_o) increased with an increase in net confining stress. The IC tests indicated the strong influence of matric suction on compressibility and stiffness of the compacted kaolin. The results of SI tests indicated that water infiltration reduced the matric suction of the soil and was accompanied by a degradation in deviator stress. It was also found from the CD and SI tests that the failure envelope of compacted kaolin was unique. For practical purposes of transient analyses, therefore, the CD and SI tests, as well as the SWCC and IC tests, might be performed to obtain more rigorously elastoplastic behavior of unsaturated soil under CD and SI conditions.

Keywords

elastoplastic behavior, triaxial test, compacted soil, volume change, shear strength

Manuscript received July 19, 2018; accepted for publication February 19, 2019; published online May 2, 2019. Issue published March 1, 2020.

[1] School of Civil and Environmental Engineering, Nanyang Technological University, 50 Nanyang Ave., Singapore 639798, https://orcid.org/0000-0002-8551-8022 (Y.K.)

[2] School of Civil and Environmental Engineering, Nanyang Technological University, 50 Nanyang Ave., Singapore 639798 (Corresponding author), e-mail: chrahardjo@ntu.edu.sg

Introduction

A large number of geotechnical problems involve unsaturated soil zones in which the voids between soil particles are filled with air and water. There are many practical situations associated with unsaturated soils that are challenging to geotechnical engineers in the field.

In the case that fill materials are compacted or loaded, the excess pore-air pressure during compaction or loading will dissipate immediately; meanwhile, the excess pore-water pressure will dissipate with time. During and after rainfall events, the increase in pore-water pressure and volume change that is due to infiltration may result in slope instability (Tami et al. 2004; Harnas et al. 2016; Kim, Hwang, and Kim 2018). Therefore, the influence of matric suction on shear strength, volume change, and excess pore-water pressure has been investigated under various confining stresses and matric suctions in a triaxial apparatus (Bishop et al. 1960; Blight 1961; Satija 1978; Sivakumar 1993; Fredlund and Rahardjo 1993; Wong et al. 2001; Rahardjo, Ong, and Leong 2004; Meilani, Rahardjo, and Leong 2005).

The changes in void ratio (e) and water content (w) of unsaturated soil with respect to the two independent stress state variables, net normal stress and matric suction, can be represented by constitutive equations. Numerous researchers (Bishop and Blight 1963; Fredlund and Morgenstern 1976; Alonso, Gens, and Josa 1990; Wheeler and Sivakumar 1995; Tang and Graham 2002; Chiu and Ng 2003; Leong, Agus, and Rahardjo 2004; Thu, Rahardjo, and Leong 2007a) have proposed constitutive equations for volume change of unsaturated soil. These have been presented in the form of mathematical expressions that can also be presented graphically. The volumetric behavior can be described by the relationship among the net mean stress (p), matric suction (s), and specific volume (v). Despite a growing interest in the research development for assessing the behavior of unsaturated soil, geotechnical engineers are not able to predict the elastoplastic characteristics of unsaturated soil with certain accuracies because of the difficulties associated with measuring the stress state variables in laboratory and evaluating the soil parameters in constitutive equations.

Comprehensive and fundamental laboratory studies on the evaluation of shear strength and soil parameters as affected by water infiltration have not been performed extensively in the laboratory. These limitations have hampered the study of elastoplastic behavior for unsaturated soil. The main objective of this study is to present an integrated laboratory study to characterize the mechanical behavior and failure mechanism of unsaturated soil under consolidated drained (CD) and shearing-infiltration (SI) conditions. The laboratory works consist of a soil-water characteristic curve (SWCC), isotropic consolidation (IC), CD, and SI tests. The SWCC test was conducted under different net confining stresses to consider in situ stress state, and the IC test was conducted under different matric suctions that describe the volume change characteristics of unsaturated soil with respect to two stress state variables, such as net normal stress and matric suction. The CD test was carried out under different net confining stresses and matric suctions to obtain shear strength and failure envelops for unsaturated soil. The SI test was carried out under different net confining stresses, matric suctions, and deviator stresses to investigate the effect of water infiltration on the changes in shear strength and the associated failure mechanism in unsaturated soil. In the combination of the laboratory study for assessing elastoplastic soil parameters, the procedures and results give insight to understand the elastoplastic behavior of unsaturated soil under a given condition.

Theoretical Background for Elastoplastic Behavior of Unsaturated Soil

The elastoplastic behavior of unsaturated soil can be described using five state variables: net mean stress (p), deviator stress (q), matric suction (s), specific volume (v), and specific water volume (v_w) (Alonso, Gens, and Josa 1990; Wheeler and Sivakumar 1995; Wang, Pufahl, and Fredlund 2002; Chiu and Ng 2003). An idealized variation of specific volume with respect to the stress state variables is shown in **figure 1**. The κ_s is the slope of the specific volume with respect to the matric suction curve before the yield suction (s_o). The κ is the slope of the elastic compression curve before the yield stress (p_o). The methodology to evaluate the yield suction is the same as the methodology to evaluate the yield stress using the Casagrande methodology (Rampino, Mancuso, and Vinale 2000; Thu, Rahardjo, and Leong 2007b). The λ_s is the slope of the specific volume with respect to the matric suction curve beyond the yield suction. The λ is the slope of the normally consolidated line beyond the yield stress.

FIG. 1

Idealized variation of specific volume (v) with net mean stress (p) and matric suction (s) along virgin and loading-unloading paths (Rahardjo et al. 2018): (*A*) v versus s and (*B*) v versus p.

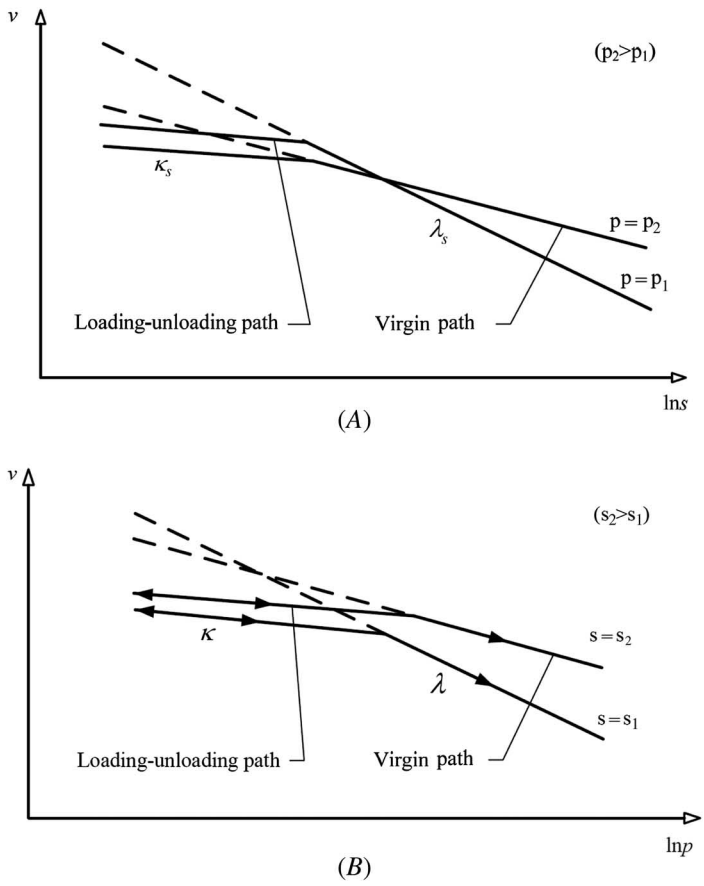

Figure 2 shows the shape of the loading-collapse (LC) and suction-increase yield curves in the $p - s$ plane. When a stress state moves from Point A to a new Point C by following the stress path ABC, the corresponding change in specific volume (Δv) can be related to the changes in net mean stress and matric suction by elastic stiffness parameters κ_s and κ, respectively. Any tendency for the stress variables of matric suction and net mean stress to move outside the initial yield surface produces a corresponding change in specific volume that is related to the changes in net mean stress and matric suction by plastic stiffness parameters λ_s and λ. The LC and suction-increase yield curves are expressed in equations (1) and (2), respectively, as proposed by Rahardjo et al. (2018).

$$[\lambda - \kappa] \ln\left(\frac{p_o}{p_{at}}\right) = [\lambda(0) - \kappa] \ln\left(\frac{p_o(0)}{p_{at}}\right) + N(s) - N(0) + \kappa_s \ln\left(\frac{s + p_{at}}{p_{at}}\right) \quad (1)$$

$$[\lambda_s - \kappa_s] \ln\left(\frac{s_o}{p_{at}}\right) = [\lambda_s(0) - \kappa_s] \ln\left(\frac{s_o(0)}{p_{at}}\right) + N_s(p) - N_s(0) + \kappa \ln\left(\frac{p + p_{at}}{p_{at}}\right) \quad (2)$$

where p_o is the mean net yield stress of unsaturated soil, p_{at} is the atmospheric pressure, $\lambda(0)$ is the plastic stiffness parameter from the normally consolidated curve (i.e., beyond the yield stress) under zero matric suction, $p_o(0)$ is the mean net yield stress at the saturated condition, $N(s)$ is the specific volume of the normal consolidation line under a given matric suction, $N(0)$ is the specific volume of the normal consolidation line under zero matric suction at atmospheric pressure, s_o is the yield suction of unsaturated soil, $s_o(0)$ is the yield suction at zero

FIG. 2

Stress paths in the elastic zone on the $p-s$ plane: (*A*) LC yield curve (modified from Alonso, Gens, and Josa 1990) and (*B*) suction increase yield curve (Rahardjo et al. 2018).

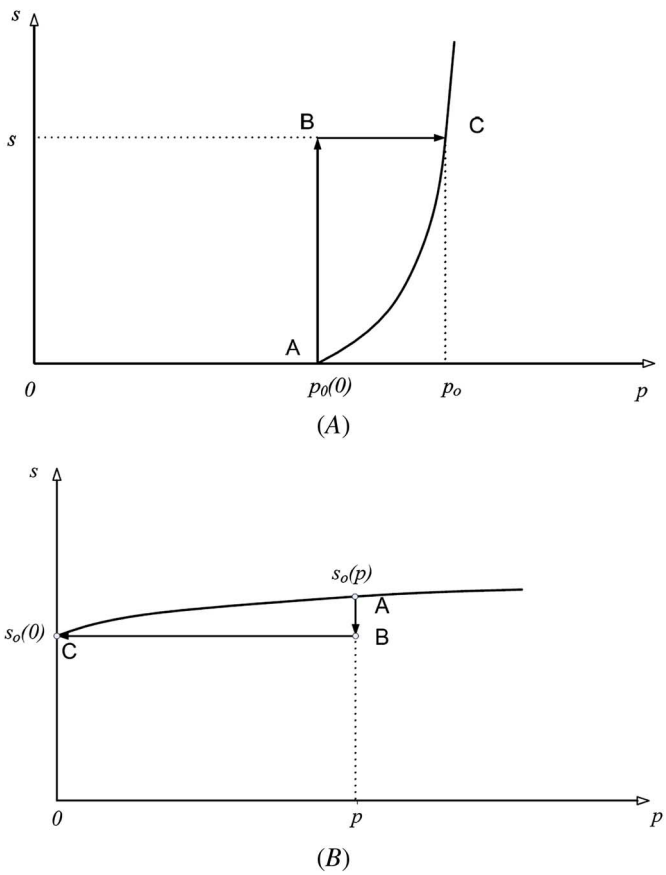

net mean stress, $\lambda_s(0)$ is the plastic stiffness parameter from the relationship between specific volume and matric suction (i.e., beyond the yield stress) under zero net mean stress, $N_s(\mathrm{p})$ is the specific volume under a given net mean stress at matric suction equal to atmospheric pressure, and $N_s(0)$ is the specific volume under a given net mean stress under zero net mean stress.

Experimental Setup

To examine the elastoplastic behavior of compacted kaolin under CD and SI triaxial conditions, comprehensive experimental tests were performed with respect to stress state variables, such as net normal stress and matric suction. The experiments included SWCC, IC, CD, and SI tests. The elastoplastic soil parameters for an elasto-plastic constitutive equation were obtained from the SWCC and IC tests. The shear strength parameters and characteristics of total volume change and water volume change were obtained from the CD tests. The stress path and the characteristics of matric suction change under infiltration were obtained from the SI tests.

TRIAXIAL SETUP

In this study, a modified triaxial apparatus was used for SWCC tests under different net confining stresses, IC tests under different matric suctions, CD triaxial tests, and SI tests. The modified triaxial apparatus consists of a triaxial cell, two digital pressure and volume controllers (DPVCs), and a diffused-air volume indicator. Both pore-air pressure and pore-water pressure in the soil specimen is controlled using the axis-translation technique

FIG. 3 Modified triaxial apparatus for unsaturated soil testing (modified from Fredlund and Rahardjo 1993)

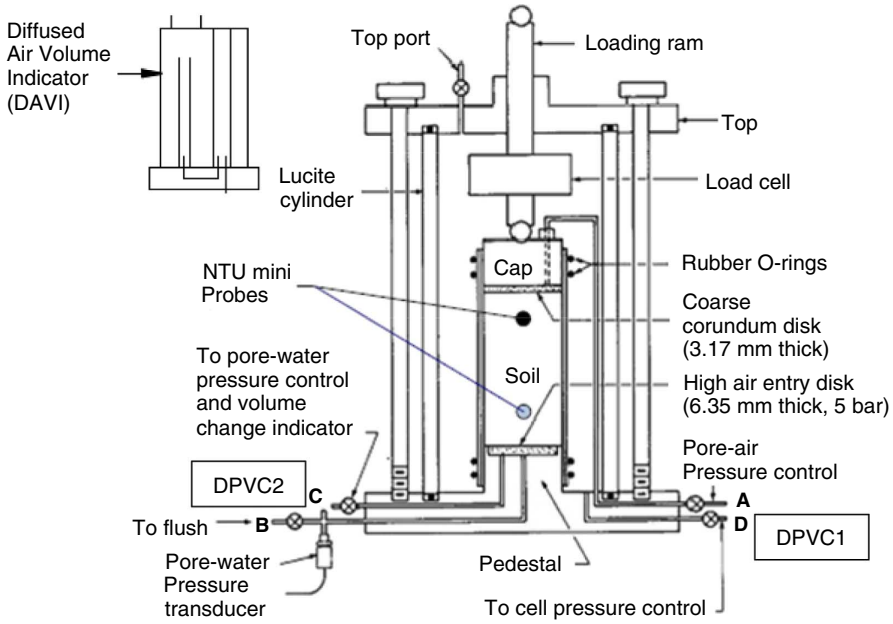

(Hilf 1956). Three Nanyang Technological University (NTU) mini suction probes were installed along the specimen to measure the pore-water pressures during testing. The modified triaxial apparatus is similar to the modified triaxial apparatus described by Fredlund and Rahardjo (1993) as shown in **figure 3**.

The confining, pore-air, and pore-water pressures were applied by opening valves D, A, and C, respectively. For the flushing process, valves B and C were opened and the air bubbles that accumulated in the water compartment were removed by the water pressure gradient. The DPVC-1 controlled the cell pressure and recorded the cell volume change. The cell volume change was used to measure the volume change of the soil specimen during the test. The DPVC-2 controlled the water pressure at the base plate. All the pressure transducers and NTU mini suction probes were calibrated before the tests started and at every 6-month period during the testing program.

To account for the effect of pressure change and creep of the Perspex cell, the cell volume change correction had been applied. The correction was determined by running a test using a dummy specimen (i.e., stainless steel). The dummy specimen has the same size as that of the soil specimen and it can be considered as having no volume change. The results from this test gave the correction for volume change measurement of the soil specimen. A data acquisition unit and a personal computer were used to automate the measurements.

SPECIMEN PREPARATION

Kaolin made by Kaolin (Malaysia) SDN BHD (Kuala Lumpur, Malaysia) was chosen for the experimental program. Identical statically compacted specimens were prepared by the standard Proctor compaction test (ASTM D698-00ae1, *Standard Test Methods for Laboratory Compaction Characteristics of Soil Using Standard Effort (12,400 ft-lbf/ft3 (600 kN-m/m3))* (Superseded)) to minimize difficulties associated with heterogeneity. The kaolin has a maximum dry density of 1.37 mg/m^3 and an optimum water content of 26.5 % as shown in **figure 4**. Based on the grain size distribution curve test (ASTM D422-63(2002), *Standard Test Method for Particle-Size Analysis of Soils* (Superseded)), the soil consists of 83.7 % silt and 16.3 % clay-size particles (finer than 2 μm).

FIG. 4

Compaction curve of kaolin.

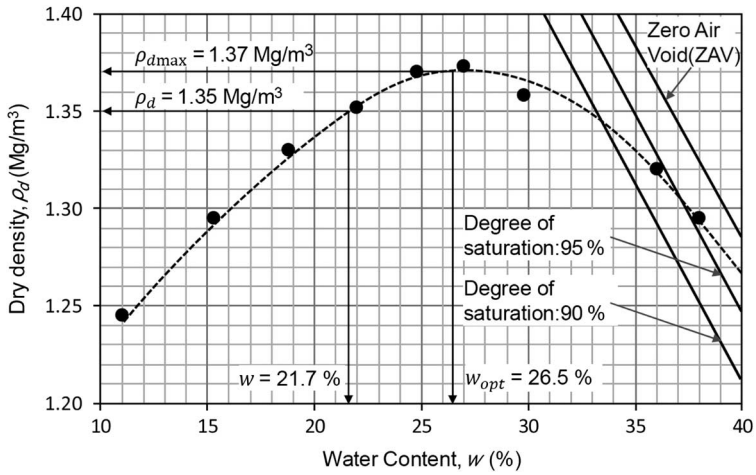

The kaolin's specific gravity of 2.68 was determined according to ASTM D854-00, *Standard Test Methods for Specific Gravity of Soil Solids by Water Pycnometer* (Superseded). The kaolin has a liquid limit of 56.1 %, a plastic limit of 37.9 %, and a plasticity index of 18.2 %. The liquid limit and plastic limit were determined according to BS 1377-2, *Methods of Test for Soils for Civil Engineering Purposes—Part 2: Classification Tests*, and ASTM D4318-00, *Standard Test Methods for Liquid Limit, Plastic Limit, and Plasticity Index of Soils* (Superseded), respectively. Based on the plasticity chart of the Unified Soil Classification System (ASTM D2487-00, *Standard Classification of Soils for Engineering Purposes (Unified Soil Classification System)*), the kaolin was classified as silt with high plasticity.

TESTING PROCEDURE

Four types of triaxial tests on saturated and unsaturated soils were carried out in accordance with the procedures proposed by Head (1986) and Fredlund and Rahardjo (1993), respectively. **Figure 5** depicts the procedures of the four triaxial tests.

FIG. 5 Schematic view of the experimental procedures for the four types of triaxial tests

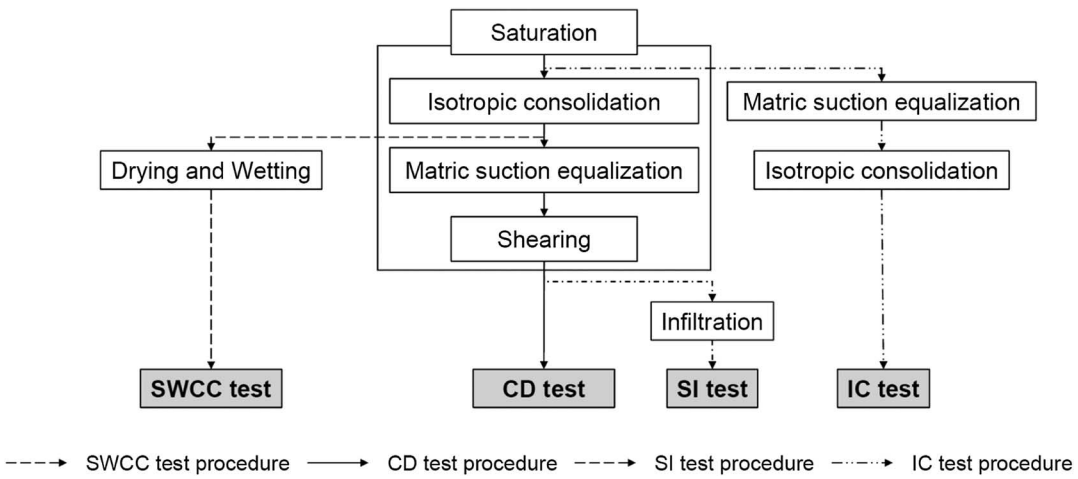

Saturation Stage

The homogeneous specimen was initially saturated. The water pressure line was connected to a digital pressure and volume controller to pump water into the specimen from the top. The specimen was saturated by applying a cell pressure and a back pressure with the difference between cell pressure and back pressure being 10 kPa. The specimen was assumed to be fully saturated when the value of B was greater than 0.97 (Head 1986).

Consolidation Stage

The soil specimen was isotropically consolidated to the required net confining stress ($\sigma_3 - u_a$) after the saturation stage. During the IC stage, the water valves were opened, and the pressures were controlled at the required values. The total volume change of the specimen during the test was calculated based on the amount of water flowing in or out of the triaxial cell. The consolidation stage was considered complete when the water volume change leveled off and the excess pore-water pressure in the specimen was fully dissipated. The matric suction was applied to the specimen when the consolidation stage had been completed.

Drying and Wetting Stage

For SWCC tests, the drying and wetting stages were carried out after the consolidation stage. The air line was connected to the air pressure system. The water pressure in the water compartment was measured by the pressure transducer that was connected to the water compartment at the base plate. The net confining stress was set to remain constant at the targeted value by controlling the cell pressure and the air pressure. During the drying stage, matric suction was increased by keeping the air pressure constant and decreasing the water pressure at the base plate. For the wetting stage, matric suction was decreased by increasing the water pressure at the base plate. The amount of water that flowed out from or into the specimen and the total volume changes of the specimen during the drying and wetting stages were measured. The matric suction was considered to be in equilibrium when the excess pore-water pressure had fully dissipated and the water volume change had decreased to 0.04 % per day (Sivakumar 1993).

Matric Suction Equalization Stage

For IC tests, the matric suction equalization was carried out after the saturation stage. For CD and SI triaxial tests, the matric suction equalization was also carried out after the consolidation stage. During the matric suction equalization stage, the cell pressure and the air pressure remained constant at the same values as their respective values at the end of the previous stage. The water pressure in the water compartment was set at the desired value. The amount of water flowing out of the soil specimen and the total volume change of the specimen were measured.

Shearing Stage

At the end of the matric suction equalization stage, the axial load was applied at a constant strain rate to shear the specimen for CD triaxial tests. The strain rate of 0.0009 mm/min had been used for CD triaxial tests on compacted specimens of the residual soil from Jurong Sedimentary Formation of Singapore (Rahardjo, Ong, and Leong 2004) and on compacted specimens of kaolin from Kaolin (Malaysia) SDN BHD (Thu, Rahardjo, and Leong 2006). The strain rate of 0.0009 mm/min. was used in this study because the selected soil had similar properties (i.e., plasticity index, coefficient of permeability) with the soil used by Rahardjo, Ong, and Leong (2004) and Thu, Rahardjo, and Leong (2006). During the shearing stage under drained condition, the valves for the water pressure line and air line were opened and maintained at the required pressures. The shearing stage was considered complete when the shear plane in the soil specimen occurred or the deviator stress ($q = \sigma_1 - \sigma_3$) reached a constant value.

Infiltration Stage

The infiltration stage started when the shearing stage had been completed. The deviator stress was maintained by the force actuator. Water was then injected into the soil specimen from the base. The rate of water injection of 0.04 mm^3/s had been used for the SI tests on compacted specimens of kaolin from Kaolin (Malaysia) SDN BHD

FIG. 6

Stress paths for the SWCC under different net confining stresses.

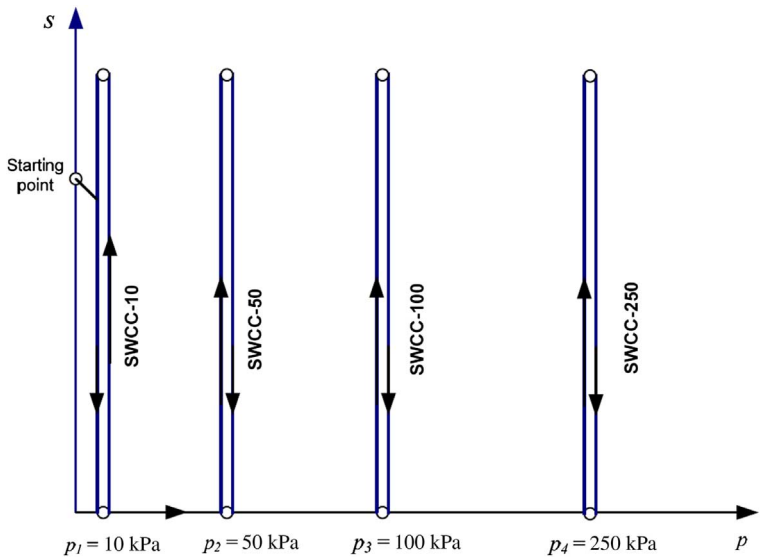

(Meilani, Rahardjo, and Leong 2005). In this study, water was injected at a rate of 0.04 mm^3/s because the selected soil had similar properties (i.e., plasticity index, coefficient of permeability) as that of the soil used by Meilani, Rahardjo, and Leong (2005). The infiltration stage was considered to be complete when the specimen had failed (Kim, Rahardjo, and Satyanaga 2017).

TESTING PROGRAM

A series of SWCC tests was conducted under different net mean stresses, $p = (\sigma_1 + \sigma_2 + \sigma_3)/3 - u_a$. The net mean stresses during the SWCC test were selected as follows: 10, 50, 100, and 250 kPa. **Figure 6** shows the stress path for the SWCC tests under different net mean stresses. Each test was named as SWCC-x where the "x" refers to the net mean stress in kPa.

The matric suction values for the IC tests were chosen as follows: 0, 30, 150, and 300 kPa. **Figure 7** shows the stress paths for the IC tests under different matric suctions. The IC test was named as IC-y where "y" refers to matric suction during the test in kPa.

The single-stage test was adopted for the CD triaxial tests. During the shearing stage, matric suction was maintained at 0, 100, or 200 kPa. **Figure 8** shows the stress paths for CD triaxial tests under difference net confining stresses and matric suctions. The CD triaxial test was named as CDxx-yy where "xx" refers to net confining stress, and "yy" refers to matric suction during the shearing stage.

The matric suction at the beginning of the shearing stage was 200 or 300 kPa. The net confining stresses at the beginning of the shearing stage were 100, 200, or 300 kPa. The specimen was sheared up to around 80 % of the peak shear stress at failure as obtained from the CD triaxial test. The independent CD triaxial test was carried out prior to the SI test to confirm the peak deviator stress of the specimen. **Figure 9** shows the stress paths for the SI tests under different net confining stresses, matric suctions, and deviator stresses.

Test Results

SWCC TESTS

The variations of specific volume, specific water volume, and volumetric water content with respect to matric suction of the specimen SWCC-100 are presented in **figure 10**. The specific volume ($v = 1 + e$) decreased as the matric

FIG. 7 Stress paths for the IC tests under different matric suctions.

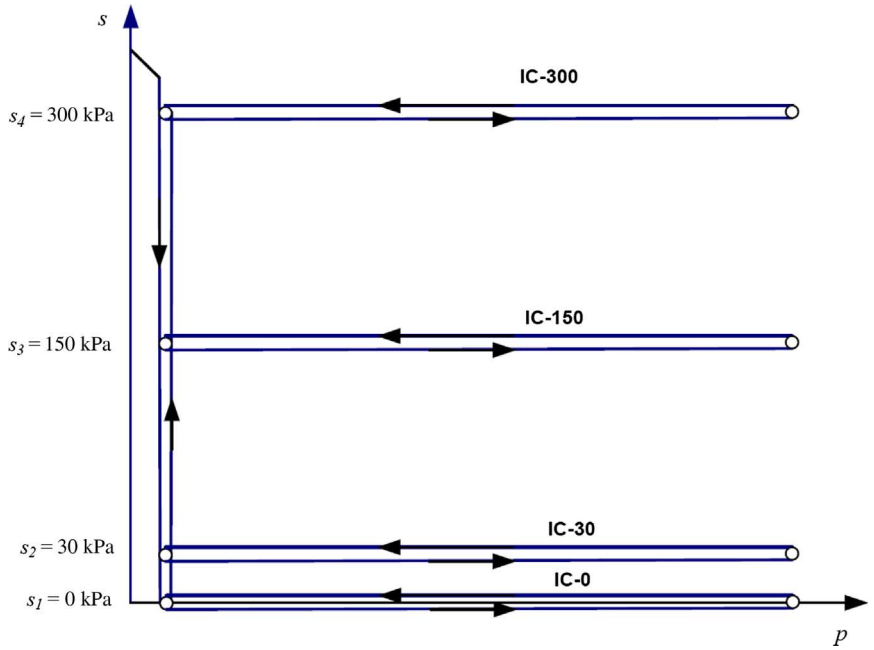

FIG. 8 Stress paths for CD tests under different net confining stress and matric suction.

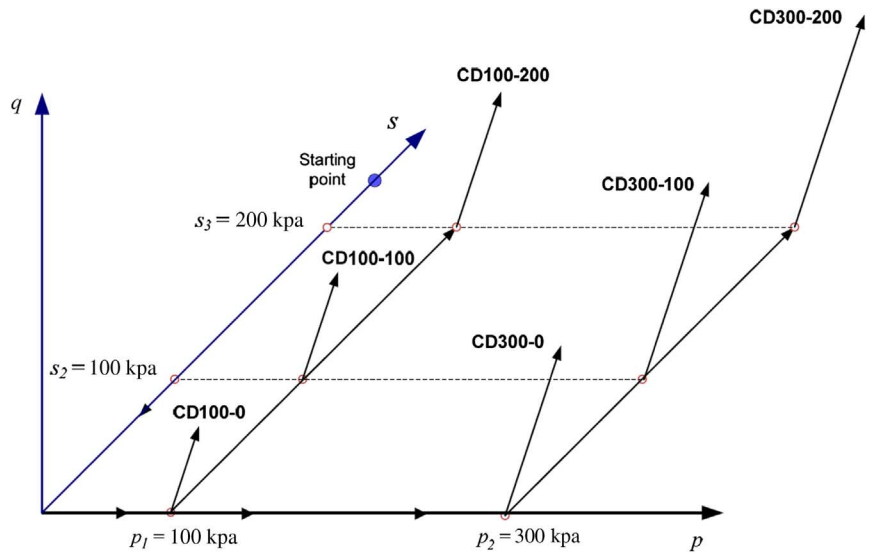

suction increased. The matric suction at the point when specific volume starts to increase drastically (i.e., inflection point) is called yield suction (s_o) of the soil (Alonso, Gens, and Josa 1990). The volumetric water content (i.e., the ratio between volume of water and total volume of soil, $\theta_w = V_w/V$) also decreased as the matric suction increased. The value of matric suction at which air first enters the pore of soil is called air-entry value (AEV).

FIG. 9

Stress paths for the SI tests under different net confining stresses, matric suctions, and deviator stresses.

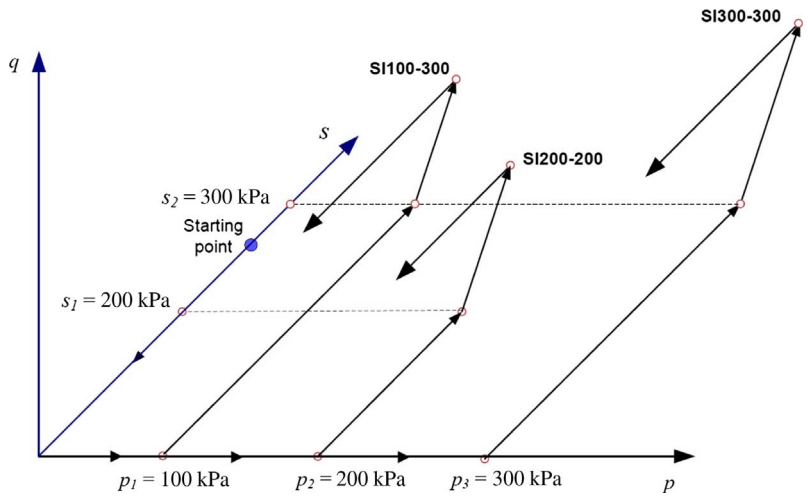

FIG. 10

Variations of volumetric water content, specific volume, and specific water volume with respect to matric suction of the specimen SWCC-100.

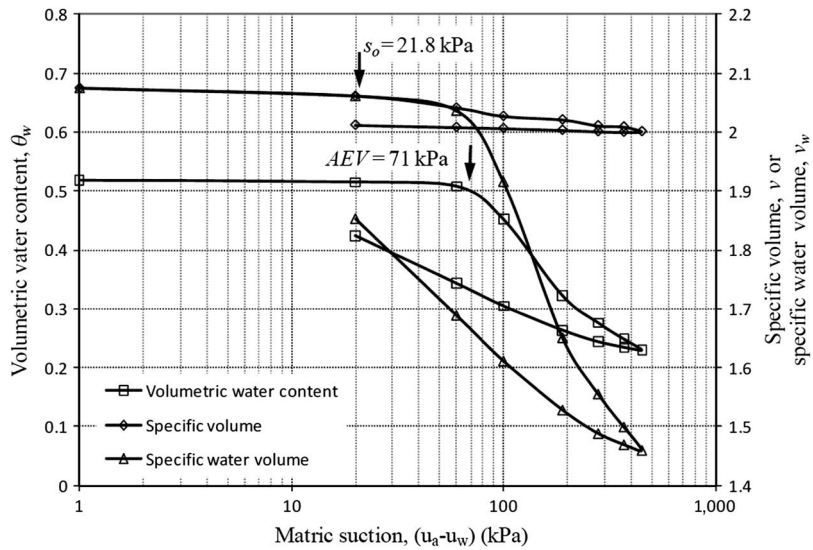

Figure 11 shows the rate of change in pore-water pressure during the drying stage under a net mean stress of 250 kPa. At the beginning of each step of the drying stage, a hydraulic head gradient developed in the ceramic disk first, and then water in the soil specimen flowed out of the soil specimen. The pore-water pressure and the volume of water in the soil specimen decreased, causing the hydraulic head gradient and the volumetric water content to decrease. The reduction of the volumetric water content leads to a reduction in the coefficient of the permeability of the soil. Therefore, the rate of change in pore-water pressure decreased because of the reduction in the hydraulic head gradient and the permeability coefficient of the soil. The figure also shows that the rate of change in pore-water pressure was dependent on the matric suction at the beginning of each step. The higher the matric suction at the beginning of the step, the lower the rate of change in pore-water pressure. This is attributed to the fact that the coefficient of permeability is dependent on the matric suction (i.e., coefficient of permeability

FIG. 11

Pore-water pressure versus elapsed time during drying stage of specimen under net mean stress of 250 kPa.

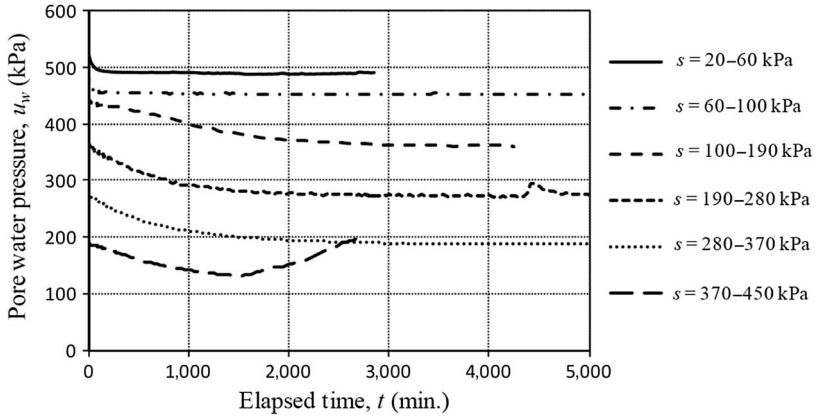

decreases with the decrease in matric suction). In addition, as the matric suction increased, the time required for pore-water pressure in the specimen to reach equilibrium increased. When matric suction increased from 370 to 450 kPa, the measurement of pore-water pressure decreased and then increased prior to reaching the equilibrium state. It was caused by the fact that good contact between the ceramic tip of suction probes and the soil specimen could no longer be maintained under the high matric suction (i.e., dryer condition). The condition may desaturate the ceramic tip and induce the suction probes to measure air pressure.

Figure 12 shows the variations of s_o and AEV with respect to net mean stress from SWCC tests. The results show that the s_o and AEV increased as net mean stresses increased. It can be said that the soil stiffness increased with the increase in net mean stresses. It could be explained that the soil specimen under a high net mean stress has a lower void ratio (e) and that the pore size of the soil specimen under the high net mean stress is smaller. A smaller pore size leads to a higher matric suction that can be maintained under a saturated condition. As a result, the AEV of the soil specimen under a higher net mean stress is higher than the AEV of the soil specimen under the lower net mean stress. Similar to the case of the AEV, the soil specimen is more compacted because of the higher net mean stress; thus the soil specimen becomes harder, resulting in a higher yield suction.

The specific volume ($N_s(p)$) on the virgin curve of the isotropic suction consolidation curve (i.e., the specific volume versus matric suction curve obtained from SWCC tests) at reference matric suction of 100 kPa also varies with net mean stresses as shown in figure 13. The $N_s(p)$ decreased with the increase in net mean stress and had a

FIG. 12

AEV and yield suction at different net mean stresses from isotropic suction consolidation curves.

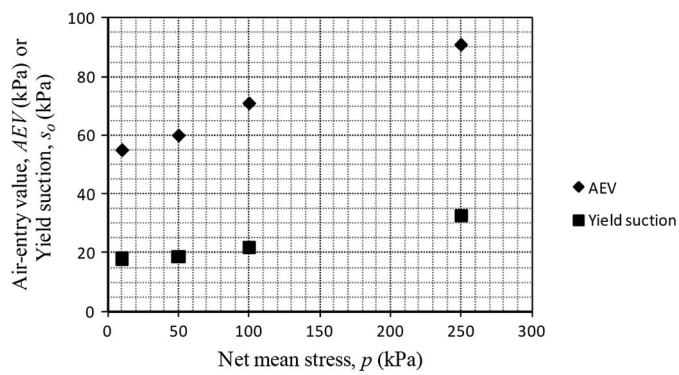

FIG. 13

Measured values of specific volume at various net mean stresses from SWCCs.

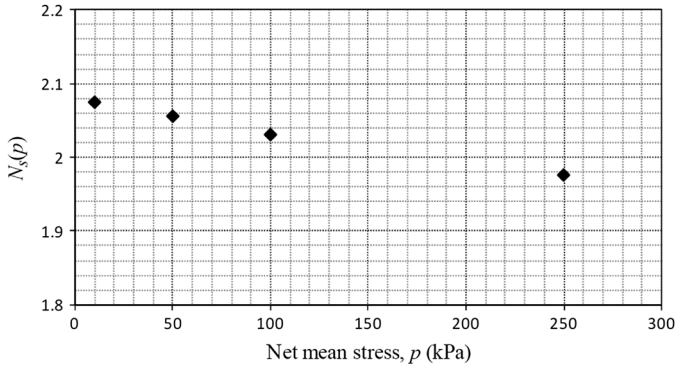

FIG. 14

Slope of virgin curve and unloading/reloading curve at various net mean stresses from isotropic suction consolidation curves.

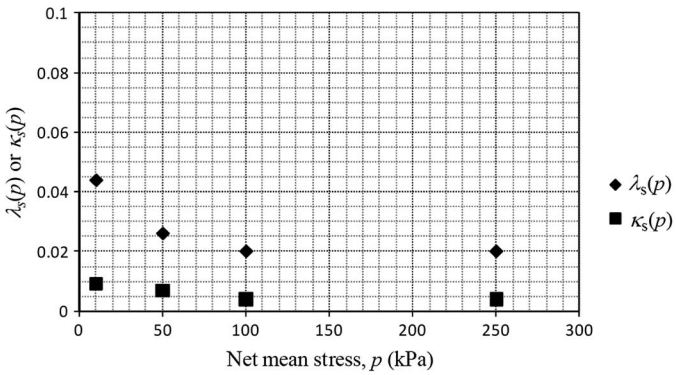

TABLE 1

Summary of soil parameters obtained from SWCC tests

Net Mean Stress, p (kPa)	AEV (kPa)	N_s (p)	λ_s (p)	κ_s (p)	s_o (kPa)
10	55	2.075	0.044	0.009	18.0
50	60	2.056	0.026	0.007	18.5
100	71	2.031	0.020	0.004	21.8
250	91	1.976	0.020	0.004	32.5

value of 2.075 at a net mean stress of 10 kPa. The change in slope of the virgin curve ($\lambda_s(p)$) of the isotropic suction consolidation curve with respect to net mean stress is shown in figure 13. The $\lambda_s(p)$ decreased with the increase in net mean stress and had a value of 0.044 at net mean stress of 10 kPa. The slopes of the unloading/reloading curves ($\kappa_s(p)$) of the isotropic suction consolidation curves are also shown in figure 14. Similar to the case of $\lambda_s(p)$ and $\lambda_s(p)$, the $\kappa_s(p)$ decreased with the increase in net mean stress. Soil parameters obtained from SWCC tests are summarized in Table 1.

IC TESTS

The variation of specific volume ($v = 1 + e$) and specific water volume ($v_w = 1 + Se$) with respect to net mean stress at various matric suctions as obtained from IC tests are shown in figures 15 and 16, respectively. The

FIG. 15

Specific volume versus net mean stresses at different matric suctions.

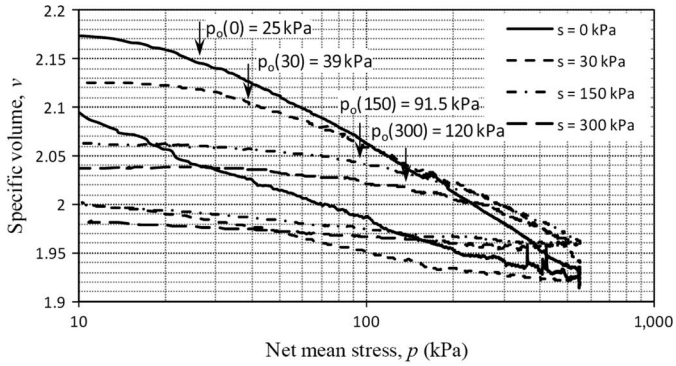

FIG. 16

Specific water volume versus net mean stresses at different matric suctions.

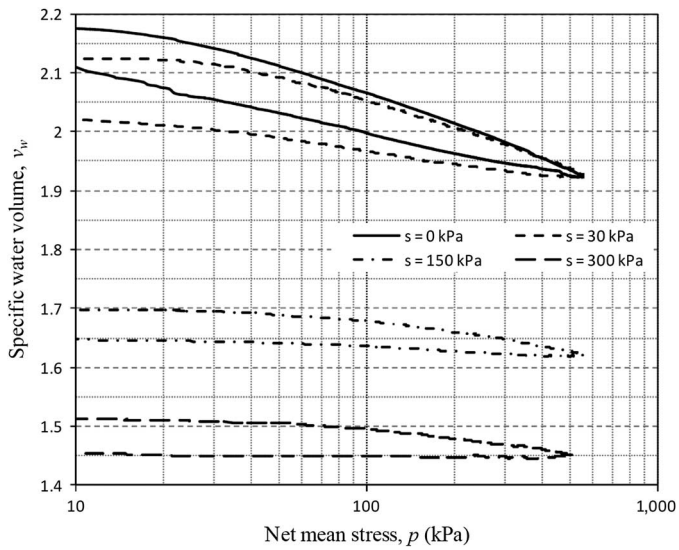

results show that the compressibility of the soil specimen decreased with the increase in matric suction. This could be attributed to the decreasing amount of water in the soil specimen with the increase in matric suction. As a result, the thickness of the water layer around the soil particle inside the soil specimen was reduced with the increase in matric suction. On the other hand, when matric suction was applied to the specimen, the void ratio decreased (i.e., soil specimen became denser), and the interforce between soil particles increased, preventing the soil particles from movement, resulting in a denser soil structure configuration. The results also indicate that the specific volume decreased rapidly when the net mean stress reached yield stress that increased gradually as the matric suction increased. It can be said that the soil stiffness increased with the increase in matric suction.

Figure 17 shows that the specific volume on the normal consolidation curve at the reference net mean stress of 100 kPa (i.e., $N(s)$) varied with matric suction. The reference mean net stress of 100 kPa was adopted by Wheeler and Sivakumar (1995) and Thu, Rahardjo, and Leong (2007b). In a saturated condition, the $N(s)$ has a value of 2.052. The $N(s)$ decreased slightly with the increase in matric suction. Similarly, the specific water

FIG. 17

Changes in specific volume ($N(s)$) and specific water volume ($N_w(s)$) at various matric suctions from IC curves.

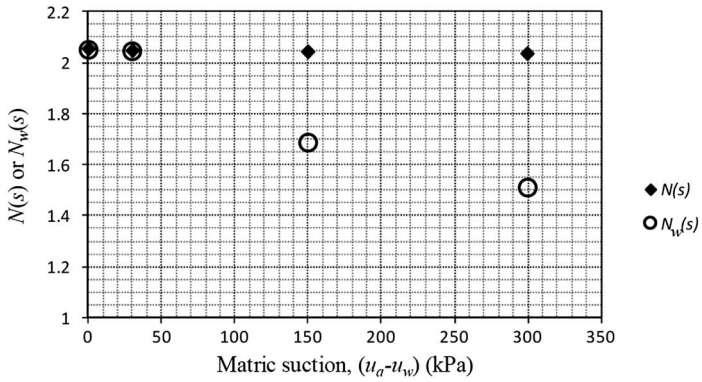

FIG. 18

Slope of normal consolidation curves and unloading/reloading curves at various matric suction as obtained from IC curves.

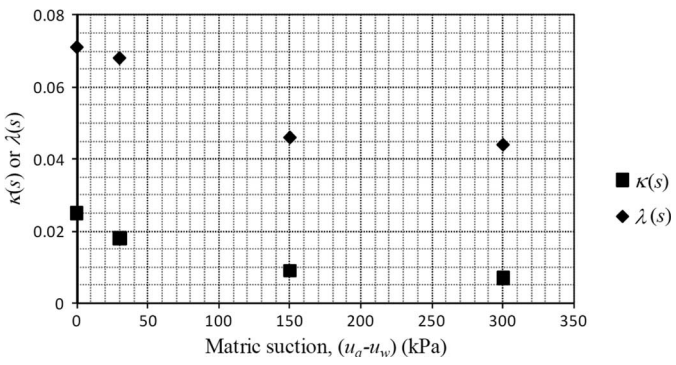

volume at the reference net mean stress of 100 kPa in saturated condition (i.e., $N_w(0)$) has a value of 2.052. The $N_w(s)$ also decreased with the increase in matric suction.

Figure 18 shows changes in the slope of the normal consolidation curve ($\lambda(s)$) with respect to matric suction. At saturation condition, the value of the slope of the consolidation curve ($\lambda(0)$) is 0.071 and the ($\lambda(s)$) decreased with the increase in matric suction. It was also found that the slopes of unloading/reloading curves (($\kappa(s)$) of the IC curves decreased with the increase in matric suction as shown in figure 17. Similarly, for specific water volume, the variations of the measurement values of $\kappa_w(s)$ and $\lambda_w(s)$ with respect to matric suction are shown in figure 19, decreasing with the increase in matric suction. The parameters obtained from the IC tests are summarized in Table 2. Note that similar trends concerning the effect of matric suction on soil parameters were observed by Wheeler and Sivakumar (1995) and Thu, Rahardjo, and Leong (2007b) in their laboratory tests.

CD TRIAXIAL TESTS

Figure 20 shows the variation of deviator stress ($q = \sigma_1 - \sigma_3$) with respect to axial strain (ε_a) during the shearing stage under different matric suctions (i.e., 0, 100, and 200 kPa) and net confining stresses (i.e., 100 and 300 kPa). The results show that the stiffness of the compacted kaolin increased with the increase in both net confining stress and matric suction. The deviator stresses with relatively lower net confining stress exhibited a rapid decrease after

FIG. 19

Measured values of $\kappa_w(s)$ and $\lambda_w(s)$ at various matric suction as obtained from IC tests.

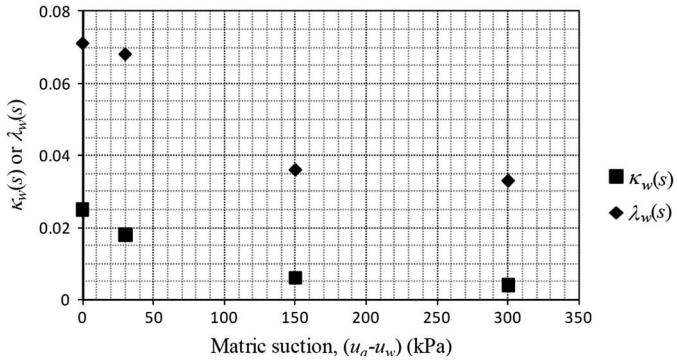

TABLE 2

Summary of parameters obtained from the IC tests

Matric Suction, s (kPa)	p_o (kPa)	$\kappa(s)$	$\lambda(s)$	$N(s)$	$\kappa_w(s)$	$\lambda_w(s)$	$N_w(s)$
0	25	0.025	0.071	2.052	0.025	0.071	2.052
30	39	0.018	0.068	2.045	0.018	0.068	2.045
150	91	0.009	0.046	2.041	0.006	0.036	1.685
300	120	0.007	0.044	2.034	0.004	0.033	1.507

the peak value. On the other hand, the deviator stresses with relatively higher net confining stress did not drop significantly after the peak value.

Figure 21 shows the variation of volumetric strain (ε_v) with respect to axial strain during the shearing stage under different net confining stresses (i.e., 100 and 300 kPa) and matric suctions (i.e., 0, 100, 200 kPa). The results show that the higher the net confining stress, the higher the compression will be. Figure 21*A* shows that the specimens tested under the same net confining stress of 100 kPa and at different matric suction compressed first until the axial strain reached around 4 % then remained constant until the axial strain reached 6 % and then dilated afterwards. On the other hand, figure 21*B* shows that specimens tested under the same net confining stress of 300 kPa and at different matric suctions compressed and reached a constant volume (i.e., reached the critical state) during the shearing stage. This is attributed to the higher net confining stresses that resulted in more compression (or less dilation) of the soil during shearing.

To investigate the failure criterion of compacted kaolin based on CD triaxial tests, the peak deviator stresses from the relationship between deviator stress and axial strain as shown in figure 20 were used in this study. The peak deviator stresses as a failure criterion and the extended Mohr-Coulomb failure envelope for the CD triaxial tests are illustrated in figures 22 and 23, respectively. The deviator stresses and axial strains at failure increased with the increase in net mean confining stress under the same matric suction and increased with the increase in matric suction under the same net mean confining stress. The axial strain increased to 6 % when the deviator stress reached around 90 % of the peak deviator stress. After that, the deviator stresses increased slowly to reach the peak deviator stress and then decreased slowly, except for the case of CD 100-100 and CD 100-200 triaxial tests. The rapid decrease in deviator stress with respect to axial strain for the CD 100-100 and CD 100-200 could be due to the brittle failure mode that occurred in those specimens. The shear strength parameters obtained from figure 23 indicate that the effective cohesion increased with the increase in matric suction, whereas the effective internal friction angle remained constant during the tests. Table 3 summarizes the values of deviator stress, axial strain, effective internal friction angle, and effective cohesion at failure.

FIG. 20

Variation of deviator stresses with respect to axial strain from CD triaxial test under the different net confining stresses and matric suctions of 0, 100, and 200 kPa. (*A*) Net confining pressure of 100 kPa. (*B*) Net confining pressure of 300 kPa

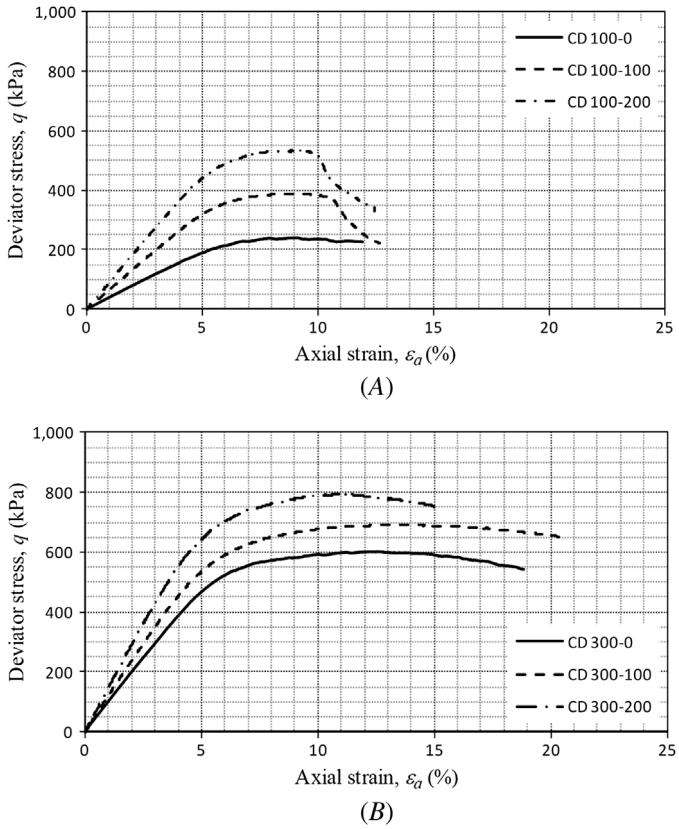

SI TRIAXIAL TESTS

Figure 24*A* shows the reduction in deviator stress in specimen SI 200-200 during the shearing and infiltration stages. During the infiltration stage, the deviator stress dropped and the specimen started to fail. The deviator stress could not be maintained and gradually decreased after failure occurred. Figure 24*B* illustrates the volumetric strain during the shearing and infiltration stages. During the shearing stage, the specimen was subjected to compression because water drained out from the specimen. On the other hand, dilation was induced during the infiltration stage when water was injected from the bottom of the specimen. Figure 24*C* shows the variation in matric suction in response to changes in axial strain (ε_a). The reading demonstrates that matric suction remained constant during the shearing process. Note that the pore-air and pore-water pressure were under drained conditions during the shearing stage. During the infiltration stage, matric suction decreased at the beginning of the infiltration stage without the change in axial strain, then the rate of change in the axial strain with respect to matric suction increased exponentially. Failure was deemed to occur when the rate of change in the axial strain with respect to matric suction increased rapidly. Figure 25 shows the failure envelope from the CD triaxial tests and the stress paths from SI tests on unsaturated specimens at the same net mean confining stress. The figures indicate that all the stress paths of specimens from the SI tests reached the failure envelopes accompanied by decreasing the matric suction during the infiltration stage. It can be said that the failure envelopes obtained from the CD and SI tests appear to be the same. Similar results concerning the failure envelope of unsaturated soil were found by Rahardjo et al. (2009) in their experimental study.

FIG. 21

Variation of volumetric strain with respect to axial strain from CD triaxial test under different net confining stresses and matric suctions of 0, 100, and 200 kPa. (*A*) Net confining pressure of 100 kPa. (*B*) Net confining pressure of 300 kPa

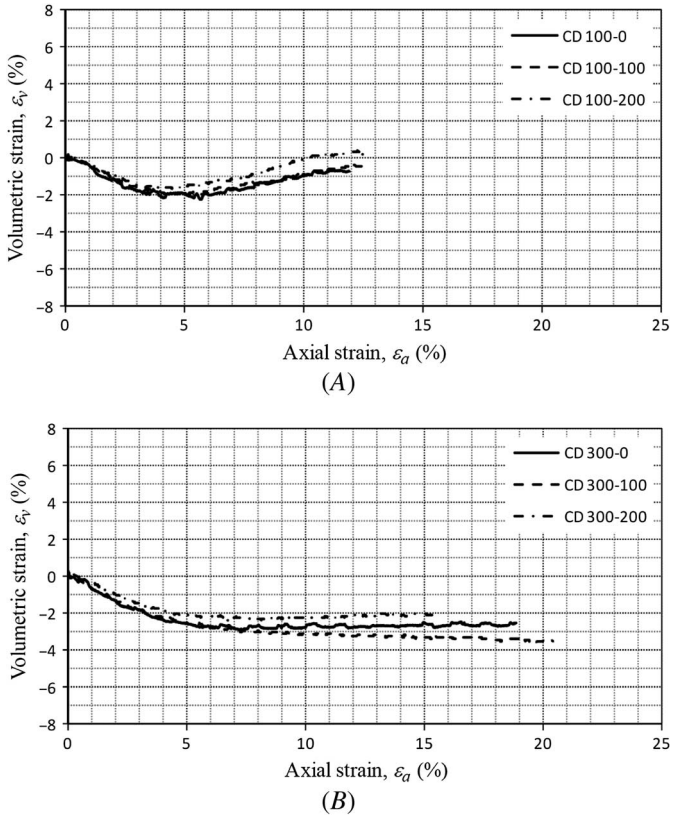

FIG. 22

Peak deviator stresses of the CD triaxial tests under different matric suctions of 0, 100, and 200 kPa and net confining stresses of 100 and 300 kPa.

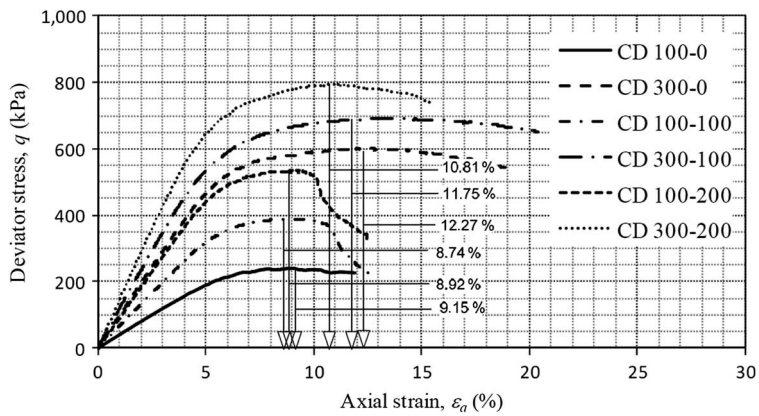

Discussions

The stress paths of SWCC tests on compacted kaolin specimens are shown in figure 6. The IC test on the compacted kaolin at a matric suction of 0 kPa (i.e., saturated condition) shows that the yield stress ($p_o(0)$) had a value

FIG. 23 Extended Mohr-Coulomb failure envelope for CD triaxial tests.

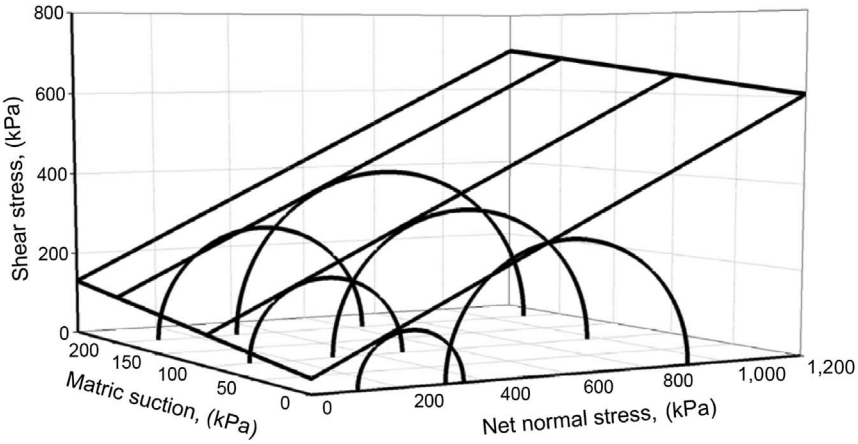

TABLE 3
Summary of deviator stresses and axial strains at failure for the CD triaxial tests

Specimen	Deviator Stress at Failure, q_f (kPa)	Axial Strain, ε_{af} (%)	Effective Internal Friction Angle, ϕ' (°)	Effective Cohesion, c' (kPa)
CD 100-0	242.05	9.15	25.6	33.3
CD 300-0	601.75	12.27		
CD 100-100	373.21	8.74	25.6	72.0
CD 300-100	648.65	11.75		
CD 100-200	534.19	8.92	25.6	110.6
CD 300-200	793.56	10.81		

of 25 kPa. Therefore, plastic strain developed during the consolidation stage of the SWCC-50, SWCC-100, and SWCC-250 tests. The stress paths for the IC tests on the compacted kaolin are shown in figure 7. The SWCC test at a net mean stress of 10 kPa (i.e., SWCC-10) gave a yield suction of 18 kPa. Therefore, plastic strains developed during the matric suction equalization stage of the IC-30, IC-150, and IC-300 tests.

The variations of deviator stress with respect to axial strain during the shearing stage under CD condition (fig. 20) show that under the same net confining stress, the peak deviator stress increased with the increase in matric suction. In other words, the shear strength increased with the increase in matric suction. It can be seen from figure 22 that the axial strain increased to 6 % when the deviator stress reached around 90 % of the peak deviator stress. After that, the deviator stresses increased slowly to reach the peak deviator stress and then decreased slowly, except for the case of CD 100-100 and CD 100-200 triaxial tests. The rapid decrease in deviator stress with respect to axial strain for the CD 100-100 and CD 100-200 tests could be due to the brittle failure mode that occurred in those specimens.

Figure 26 shows the variations of matric suction with respect to axial strain during the shearing stage of specimens tested under different initial matric suctions and net confining stresses. It could be seen that matric suction decreased by up to 3 kPa when the axial strain increased to 0.8 % and afterward the matric suction increased and finally reached the initial matric suction at the end of the shearing stage.

The stress paths of CD triaxial tests are shown in figure 8. The results of the SWCC tests show that plastic strain occurred during the consolidation stage and the matric suction equalization stage. As a result, the soil specimens at the beginning of the shearing stage were normally consolidated. Therefore, the behavior of soil specimens during the shearing stage could resemble that of the normally consolidated soil behavior. The results from specimens tested under a net confining stress of 300 kPa and at different matric suctions showed good

FIG. 24

Results of SI tests of compacted kaolin under net confining stress of 200 kPa and matric suction of 200 kPa: (*A*) variation of deviator stress, (*B*) variation of volumetric strain, and (*C*) variation of matric suction

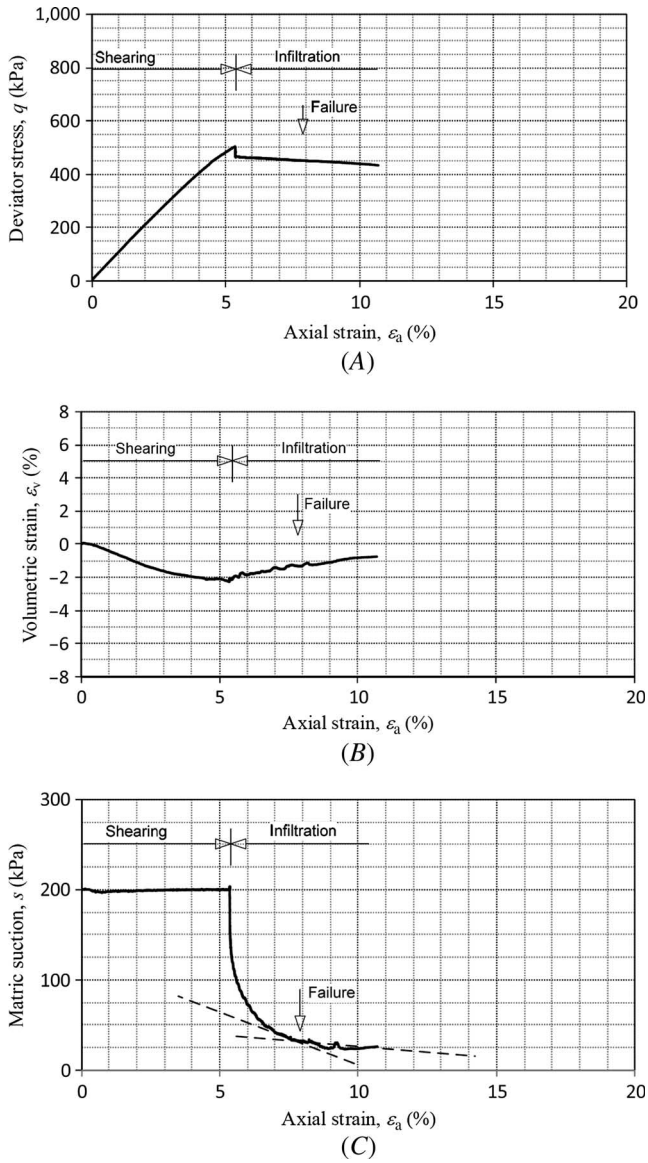

agreement with the behavior of normally consolidated soil. However, there was a small difference in the normally consolidated soil behavior for the specimens tested under a net confining stress of 100 kPa and at different matric suctions. The difference was that the soil specimens dilated when the axial strain became greater than 6 %. The reason for this difference can be explained as follows: when the axial strain reached 6 %, the deviator stress reached around 90 % of the peak deviator stress. Because of the low net confining stress, the movement of soil particles could lead to the opening of microcracks that started to develop inside the specimen. As a result, the total volume of the specimen increased. In the case of the CD 100-100 and CD 100-200 tests, it can be said that the volumetric strain versus axial strain curve was valid only before the axial strain reached 6 % because the pore size continued to decrease during the shearing stage and the opening of microcracks continued to develop inside the specimen. In general, the opening and development of microcracks occurred inside the specimen tested under a low net confining stress when the deviator stress increased to a magnitude greater than 90 % of the peak deviator stress.

FIG. 25

Failure envelope and stress path of SI tests on $q - s$ plane. (*A*) SI 100-300. (*B*) SI 200-200. (*C*) SI 300-300.

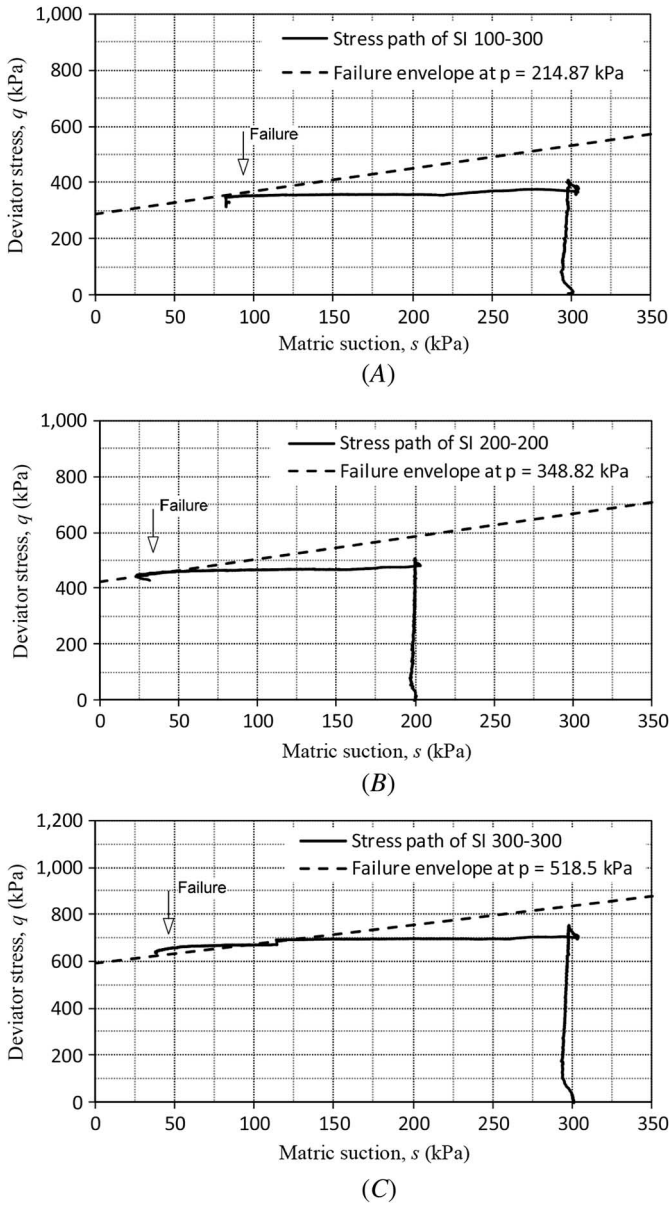

The stress paths of specimens SI 100-300 and SI 200-200 reached the failure envelope, and the failure points were also close to the failure envelope as shown in **figure 25*A*** and **25*B***. However, the stress path of Specimen SI 300-300 (**fig. 25*C***) exceeded the failure envelope, and the failure point was above the failure envelope. This could be due to the interruption of electricity in the laboratory.

Conclusions

A series of laboratory tests was conducted to characterize the elastoplastic behavior of unsaturated soil under the CD and SI conditions. The following conclusions have been obtained:

FIG. 26

Variation of matric suction with respect to axial strain during shearing stage of specimen CD 100-100 and CD 300-100.

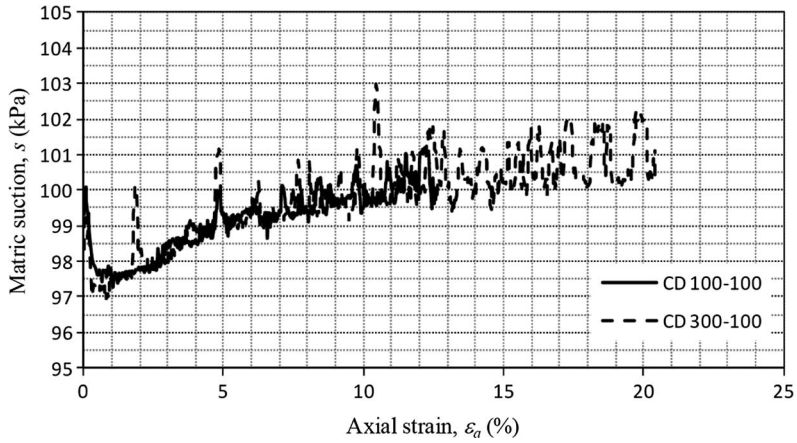

1. The yield suctions obtained from the SWCC tests increased with the increase in net mean stress. On the other hand, the slopes of the isotropic suction consolidation curve (i.e., slope of the unloading/reloading curve and slope of the virgin curve) decreased with the increase in net mean stress. In addition, the AEVs increased with the increase in net mean stress.
2. The yield stresses obtained from the IC tests increased with the increase in matric suction. The slopes of the IC curve decreased with the increase in matric suction. During the loading stage of the IC tests, the specific volume of compacted soil specimens decreased, the matric suction was smaller than the initially applied matric suction, and water flowed out of the specimens. On the other hand, during the unloading stage of the IC tests, the specific volume of compacted soil specimens increased, the matric suction was higher than the initially applied matric suction, and water flowed into the specimens.
3. Matric suction obtained from the CD tests during the shearing stage was smaller than the initially applied matric suction. This was in agreement with the variation of water volume change during the shearing stage (i.e., water volume change decreased throughout the shearing stage). The behavior of compacted soil specimens was similar to the behavior of the normally consolidated soil. In other words, the total volume change of specimens should decrease throughout the shearing stage.
4. Matric suction obtained from the SI tests decreased during the infiltration stage that caused the degradation of deviator stresses. The stress path of the SI tests reached the failure envelope, and the failure points were also close to the failure envelope obtained from the CD tests. It could be said that the failure envelopes obtained from the CD and SI tests appeared to be similar.
5. For practical purposes of transient analyses of slope, the CD and SI tests as well as the SWCC and IC tests will have to be performed in order to examine more rigorously the elastoplastic behavior of unsaturated soil under CD and SI conditions.

References

Alonso, E. E., A. Gens, and A. Josa. 1990. "A Constitutive Model for Partially Saturated Soils." *Géotechnique* 40, no. 3 (September): 405–430. https://doi.org/10.1680/geot.1990.40.3.405

ASTM International. 2000. *Standard Classification of Soils for Engineering Purposes (Unified Soil Classification System)*. ASTM D2487-00. West Conshohocken, PA: ASTM International. https://doi.org/10.1520/D2487-00

ASTM International. 2002. *Standard Test Method for Particle-Size Analysis of Soils* (Superseded). ASTM D422-63(2002). West Conshohocken, PA: ASTM International. https://doi.org/10.1520/D0422-63R02

ASTM International. 2000. *Standard Test Methods for Liquid Limit, Plastic Limit, and Plasticity Index of Soils* (Superseded). ASTM D4318-00. West Conshohocken, PA: ASTM International. https://doi.org/10.1520/D4318-00

ASTM International. 2000. *Standard Test Methods for Laboratory Compaction Characteristics of Soil Using Standard Effort (12, 400 ft-lbf/ft^3(600 kN-m/m^3))* (Superseded). ASTM D698-00ae1. West Conshohocken, PA: ASTM International. https://doi.org/10.1520/D0698-00

ASTM International. 2000. *Standard Test Methods for Specific Gravity of Soil Solids by Water Pycnometer* (Superseded). ASTM D854-00. West Conshohocken, PA: ASTM International. https://doi.org/10.1520/D0854-00

Bishop, A. W., I. Alpan, G. E. Blight, and I. B. Donald. 1960. "Factors Controlling the Shear Strength of Partly Saturated Cohesive Soil." In *Research Conference on Shear Strength of Cohesive Soils*, 503–532. Reston, VA: American Society of Civil Engineers.

Bishop, A. W. and G. E. Blight. 1963. "Some Aspects of Effective Stress in Saturated and Partly Saturated Soils." *Géotechnique* 13, no. 3 (September): 177–197. https://doi.org/10.1680/geot.1963.13.3.177

Blight, G. E. "Strength and Consolidation Characteristics of Compacted Soil." PhD diss., Imperial College London, 1961.

British Standards Institution. 1990. *Methods of Test for Soils for Civil Engineering Purposes—Part 2: Classification Tests*. BS 1377-2. London: British Standards Institution.

Chiu, C. F. and C. W. W. Ng. 2003. "A State-Dependent Elasto-Plastic Model for Saturated and Unsaturated Soils." *Géotechnique* 53, no. 9 (November): 809–829. https://doi.org/10.1680/geot.2003.53.9.809

Fredlund, D. G. and N. R. Morgenstern. 1976. "Constitutive Relations for Volume Change in Unsaturated Soils." *Canadian Geotechnical Journal* 13, no. 3 (August): 261–276. https://doi.org/10.1139/t76-029

Fredlund, D. G. and H. Rahardjo. 1993. *Soil Mechanics for Unsaturated Soils*. Hoboken, NJ: John Wiley & Sons.

Harnas, F. R., H. Rahardjo, E. C. Leong, and J. Y. Wang. 2016. "Physical Model for the Investigation of Capillary Barriers Performance Made Using Recycled Asphalt." *Geotechnical Testing Journal* 39, no. 6 (November): 977–990. https://doi.org/10.1520/GTJ20150084

Head, K. H. 1986. *Manual of Soil Laboratory Testing, Volume 3: Effective Stress Tests*. London: Pentech Press.

Hilf, J. W. "An Investigation of Pore-Water Pressure in Compacted Cohesive Soils." PhD diss., University of Colorado, 1956.

Kim, J., W. Hwang, and Y. Kim. 2018. "Effects of Hysteresis on Hydro-Mechanical Behavior of Unsaturated Soil." *Engineering Geology* 245 (November): 1–9. https://doi.org/10.1016/j.enggeo.2018.08.004

Kim, Y., H. Rahardjo, and A. Satyanaga. 2017. "Numerical Simulations of Triaxial Shearing-Infiltration Tests." *Soils and Foundations* 58, no. 2 (April): 398–411. https://doi.org/10.1016/j.sandf.2018.02.009

Leong, E. C., S. S. Agus, and H. Rahardjo. 2004. "Volume Change Measurement of Soil Specimen in Triaxial Test." *Geotechnical Testing Journal* 27, no. 1 (January): 47–56. https://doi.org/10.1520/GTJ10704

Meilani, I., H. Rahardjo, and E. C. Leong. 2005. "Pore-Water Pressure and Water Volume Change of an Unsaturated Soil under Infiltration Conditions." *Canadian Geotechnical Journal* 42, no. 6 (December): 1509–1531. https://doi.org/10.1139/t05-066

Rahardjo, H., I. Meilani, R. B. Rezaur, and E. C. Leong. 2009. "Shear Strength Characteristics of a Compacted Soil under Infiltration Conditions." *Geomechanics and Engineering* 1, no. 1 (March): 35–52. https://doi.org/10.12989/gae.2009.1.1.035

Rahardjo, H., B. H. Ong, and E. C. Leong. 2004. "Shear Strength of a Compacted Residual Soil from Consolidated Drained and Constant Water Content Triaxial Tests." *Canadian Geotechnical Journal* 41, no. 3 (June): 421–436. https://doi.org/10.1139/t03-093

Rahardjo, H., N. C. Thang, Y. Kim, and E.-C. Leong. 2018. "Unsaturated Elasto-Plastic Constitutive Equations for Compacted Kaolin under Consolidated Drained and Shearing-Infiltration Conditions." *Soils and Foundations* 58, no. 3 (June): 534–546. https://doi.org/10.1016/j.sandf.2018.02.019

Rampino, C., C. Mancuso, and F. Vinale. 2000. "Experimental Behaviour and Modelling of an Unsaturated Compacted Soil." *Canadian Geotechnical Journal* 37, no. 4 (August): 748–763. https://doi.org/10.1139/t00-004

Satija, B. S. "Shear Behaviour of Partially Saturated Soils." PhD diss., Indian Institute of Technology, 1978.

Sivakumar, V. "A Critical State Framework for Unsaturated Soil." PhD diss., University of Sheffield, 1993.

Tami, D., H. Rahardjo, E. C. Leong, and D. G. Fredlund. 2004. "A Physical Model for Sloping Capillary Barriers." *Geotechnical Testing Journal* 27, no. 2 (March): 173–183. https://doi.org/10.1520/GTJ11431

Tang, G. X. and J. Graham. 2002. "A Possible Elastic-Plastic Framework for Unsaturated Soils with High Plasticity." *Canadian Geotechnical Journal* 39, no. 4 (August): 894–907. https://doi.org/10.1139/t02-024

Thu, T. M., H. Rahardjo, and E.-C. Leong. 2006. "Shear Strength and Pore-Water Pressure Characteristics during Constant Water Content Triaxial Tests." *Journal of Geotechnical and Geoenvironmental Engineering* 132, no. 3 (March): 411–419. https://doi.org/10.1061/(ASCE)1090-0241(2006)132:3(411)

Thu, T. M., H. Rahardjo, and E.-C. Leong. 2007a. "Elastoplastic Model for Unsaturated Soil with Incorporation of the Soil-Water Characteristic Curve." *Canadian Geotechnical Journal* 44, no. 1 (January): 67–77. https://doi.org/10.1139/t06-091

Thu, T. M., H. Rahardjo, and E.-C. Leong. 2007b. "Soil-Water Characteristic Curve and Consolidation Behavior of a Compacted Silt." *Canadian Geotechnical Journal* 44, no. 3 (March): 266–275. https://doi.org/10.1139/t06-114

Wang, Q., D. E. Pufahl, and D. G. Fredlund. 2002. "A Study of Critical State on an Unsaturated Silty Soil." *Canadian Geotechnical Journal* 39, no. 1 (February): 213–218. https://doi.org/10.1139/t01-086

Wheeler, S. J. and V. Sivakumar. 1995. "An Elasto-Plastic Critical State Framework for Unsaturated Soil." *Géotechnique* 45, no. 1 (March): 35–53. https://doi.org/10.1680/geot.1995.45.1.35

Wong, J.-C., H. Rahardjo, D. G. Toll, and E.-C. Leong. 2001. "Modified Triaxial Apparatus for Shearing-Infiltration Test." *Geotechnical Testing Journal* 24, no. 4 (December): 370–380. https://doi.org/10.1520/GTJ11134J